Influence of hydrogen-bonding configurations on the physical properties of hydrogenated amorphous silicon

C. Manfredotti, F. Fizzotti, M. Boero, P. Pastorino, P. Polesello, and E. Vittone

Dipartimento di Fisica Sperimentale, Università di Torino and INFN Sezione di Torino, via Pietro Giuria 1, I-10125 Torino, Italy

We analyzed the physical properties of hydrogenated amorphous silicon (a-Si:H) samples grown by plasma enhanced chemical vapor deposition, by means of infrared spectroscopy, mass-density, and optical measurements. We applied the usual infrared spectroscopic techniques to evaluate the amount of incorporated hydrogen and to investigate the influence of the Si-H bonding configurations on the optical and electronic properties of a-Si:H obtained by this widely used deposition process, and with parameters so chosen as to obtain films having state of the art characteristics. We carried out an exhaustive study of the different infrared absorption peaks, generally ascribed to different bonding configurations of H in Si, with a view to distinguishing the different contributions of SiH, SiH_2, $(SiH_2)_n$ to the spectral response of the material and to relating them to deposition temperature. The correlation of this infrared spectral analysis with mass-density measurements has evidenced that, for hydrogen content below 10 at. %, isolated SiH and SiH_2 bonds occur, whereas, with higher hydrogen concentrations, the formation of $(SiH_2)_n$ chains gives rise to empty cavities where hydrogen is preferentially incorporated. In addition, optical measurements show that samples deposited at temperatures below 170 °C exhibit energy gaps and defect densities, which are quite different to those expected if only the effects of SiH groups are considered.

I. INTRODUCTION

One important step towards the understanding and control of the properties of hydrogenated amorphous silicon (a-Si:H) is the determination of the way hydrogen atoms are bound to the silicon atoms of the network. At low hydrogen concentrations (≤ 10 at. %), one may expect H atoms to be mainly in the monohydride (SiH) form. This bonding arrangement favors passivation of Si dangling bonds with consequent improvement of the electronic and optical properties of the material.[1] In samples having higher hydrogen concentrations, other structural units are present, which affect the structural and the electronic features of a-Si:H films.[2-5]

One of the most direct and nondestructive techniques for determining both the hydrogen content and the bonding configuration is the infrared absorption spectroscopy. Very comprehensive studies of the vibrational spectra of a-Si:H have been carried out in the past and the assignment of the peaks to different SiH bonding configurations has been a matter of long-standing controversy.[1,6-8] The most commonly accepted model ascribes all spectral features to the vibrational modes of SiH, SiH_2, SiH_3 units, and of $(SiH_2)_n$ chains due to clusters of SiH_2 units occurring at high hydrogen concentrations.[7] Although with such a model a comprehensive interpretation of many a-Si:H features can be given, very limited experimental investigations[4,5,9,10] have been carried out to provide suitable correlation between the different Si-H bonding configurations and some macroscopic physical properties of the material obtained under conditions approaching those usually adopted.

In the literature, detailed analyses often present the optical energy gap (E_G), the gap density of states (DOS) and mass density as functions of the total hydrogen content and disregard the effects of the SiH_2 and $(SiH_2)_n$ configurations. The importance of such configurations has been pointed out, for example, by Furukawa and Matsumoto who studied samples containing many polysilane groups which were prepared by rf glow discharge of disilane at very low substrate temperatures (from 220 to 440 K).

In this paper we give, instead, the results of an experimental investigation into the influence of the SiH_2 and $(SiH_2)_n$ configurations on the optical and structural properties of a-Si:H films prepared by plasma enhanced chemical vapour deposition (PECVD) of SiH_4. The deposition parameters were so chosen as to obtain a-Si:H films having state of art characteristics.[11] The substrate temperature was the only parameter which was varied from 140 to 270 °C in order to obtain different concentrations of Si-H bonding configurations.

The hydrogen bonding configurations have been investigated by means of an accurate analysis of infrared spectra. Absorption-peak area and positions were obtained by deconvolution of the absorption spectra extracted from transmittance measurements, account being taken of optical interference due to difference in the film-substrate refractive index. The adopted fitting procedure is consistent with the widely used IR data analysis method[1] in which empirically determined corrections are introduced.[12] The total hydrogen content was evaluated by means of the integrated absorption of the 2000–2100 cm^{-1} stretching modes and with use of the proportion-

ality factors given in a previous paper[9] and confirmed by other authors[10]. The samples deposited at relatively low temperatures (140–270 °C) show remarkable increase of the bending mode peaks (840–880 cm^{-1} region) which is attributed to the formation of $(SiH_2)_n$ chains. These polysilane chains affect the microstructure and electronic properties of the material and favor the formation of microcavities, in which hydrogen incorporates preferentially, as indicated by density and optical measurements.

II. EXPERIMENTAL PROCEDURE

The a-Si:H samples analyzed in the present work were produced by a commercially available ultra high vacuum (UHV) multichamber PECVD system manufactured by MVSystem Inc. (USA) and ElettroRava S.p.A. (Italy) as described by Madan et al.[11] The system is suitable to produce any type of multilayer device avoiding cross contamination between different layers. It contains three modular UHV PECVD chambers of stainless steel construction located around a central isolation and transfer chamber which contains the transport mechanism consisting of an arm with radial and linear movement. The modular process zones are separately pumped (up to 10^{-8} mbar) and have separate gas manifolds. The distance between the electrodes in each module can be varied from 10 to 50 mm. The substrate, facing downward to avoid accumulation of dust particles, is heated by proximity by a heater placed outside vacuum to avoid contamination. Intrinsic a-Si:H films deposited using this modular multichamber UHV PECVD system installed at ElettroRava show a dark conductivity in the $10^{-11}\,\Omega^{-1}\,cm^{-1}$ range and a photoconductivity under global AM1.5 illumination of $10^{-5}\,\Omega^{-1}\,cm^{-1}$.

The most important parameter investigated was the deposition temperature, which ranged from 140 to 270 °C, whereas reactor power (3.0 ± 0.5 W), interelectrode distance (14 mm), SiH_4 flow rate (0.4 standard cubic centimeter per minute), and total gas pressure (0.8 mbar) were kept constant.[3] For optical measurements films were deposited on Corning 7059 glass and for infrared measurements on p-type high-resistivity ($\geq 100\,\Omega$ cm) 380 μm thick silicon wafers optically polished on the deposition side only. The typical film area was 2 × 2 cm^2 and thickness ranged from 1.2 to 5 μm.

Hydrogen content and the relevant bonding configurations were determined by analyzing IR absorption spectra. A Perkin Elmer Model 1710 spectrophotometer operating at room temperature and at atmospheric pressure, in the wave-number (ω) region from 400 to 4000 cm^{-1}, (i.e., 2.5–25 μm wavelength range), with a 4 cm^{-1} resolution was used for IR measurements. It was operated in the single-beam mode, in which the transmittances of the a-Si:H sample and of a reference c-Si substrate were measured in rapid succession.

In order to obtain the film absorption coefficient from the measured transmittance spectra, the sample transmittance $T_f(\omega)$ was divided by the bare-substrate transmittance $T_s(\omega)$; substrate absorption was assumed unmodified by the presence of the film. Such a procedure—

adopted by several authors[1,10,12]—allows the c-Si absorption at wavenumbers below 1200 cm^{-1} to be taken into account. However, it involves some undesirable effects; for instance, the film-substrate transmittance $T_f(\omega)$ results in some samples, larger than that of the bare substrate, $T_s(\omega)$, in the transparent region (i.e., 2400–3600 cm^{-1}) of the spectra. This may be due to imperfect matching of the sample substrate with the c-Si reference, to the presence of air in the measurement chamber, and to a low-refractive index difference between the substrate and the film, which causes interference fringes. Nevertheless, the absorption spectra of the a-Si:H can be recovered if an appropriate base line subtraction is adopted in the treatment of the transmittance data.

The said base line was fitted in the transparent region by the function,

$$\frac{1}{T_b(\omega)} = P_n(\omega) + \Gamma\,\cos(\Omega\omega + \phi)\,, \tag{2.1}$$

where $T_b(\omega)$ is the IR transmittance and $P_n(\omega)$ is an n-degree polynomial ($n = 3, 4$) whose ($n + 1$) coefficients, together with Γ, Ω, and ϕ, are free parameters, to be determined via the best fit of experimental data. The cosinusoidal term in (2.1) has been included in order to take account of multiple reflections in the film; the refractive index n and the thickness d of the film were calculated from the angular frequency Ω and amplitude Γ of the IR fringes. The polynomial in (2.1) was introduced in order to take account of the background present in all samples. The very slight curvature of the base line may be due to oxide layers at the top and bottom substrate surfaces, which generate large interference fringes. A typical result of such base line subtraction with respect to raw experimental data is shown in Fig. 1 for a typical sample.
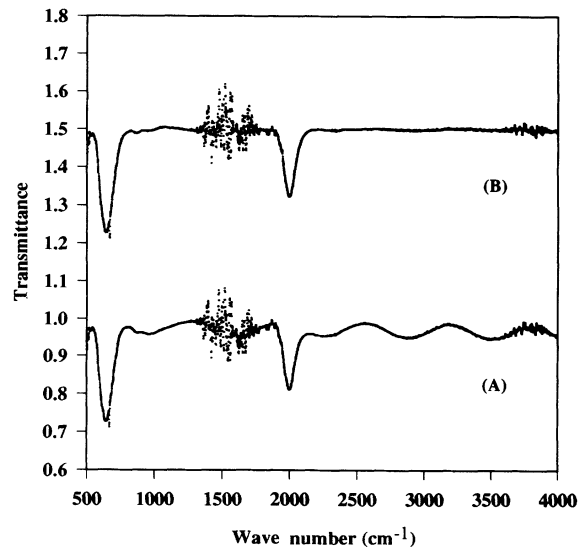
We would note that the corrected transmittance

FIG. 1. IR transmission and absorption spectra of a-Si:H deposited at the substrate temperature of 143 °C. (a) Raw experimental transmission data, (b) transmission data (shifted by 0.5) with interference effects removed.
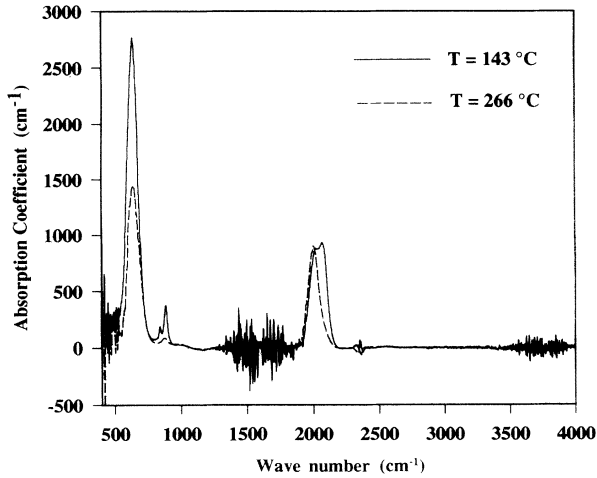
FIG. 2. IR absorption spectra of a-Si:H deposited at 143 and 266 °C. The deposition time was 150 min.

(T/T_b) is relevant to samples with non-absorbing substrates and nonreflecting substrate-film interface. Since with the method we adopted, we satisfied the conditions on which Brodsky *et al.*[1] based their approach, we calculated the absorption coefficient $\alpha(\omega)$ of the film by the formula

$$\alpha(\omega) = \frac{1}{d}\left[\ln(\mathrm{XR}) - \ln(\sqrt{1 + X^2} - 1)\right], \qquad (2.2)$$

where $X = 2R(T/T_b)/(1 - R^2)$, R is the reflectivity of silicon $(R=0.3)$[1] and d is the film thickness evaluated from the period of the interference fringes. The base line (2.1), previously evaluated only in the transparent range, has now been extended to include the whole spectrum. Figure 2 shows two absorption spectra of a-Si:H samples
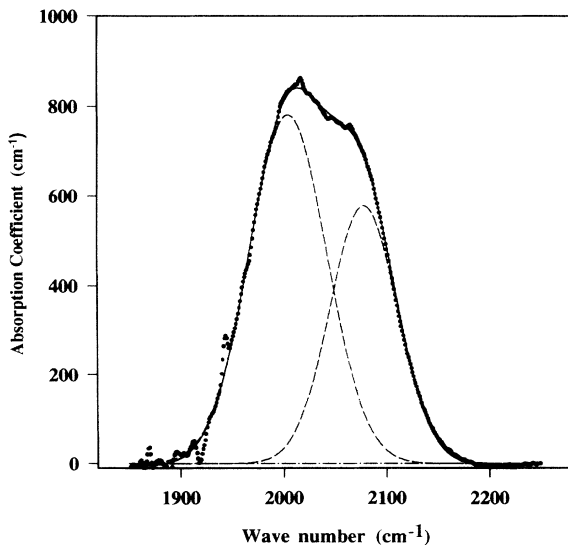

FIG. 3. Deconvolution of the 2000 and 2100 cm^{-1} stretching peaks. The two Gaussian functions are indicated by the broken lines and represent the best fit of the experimental dotted line.
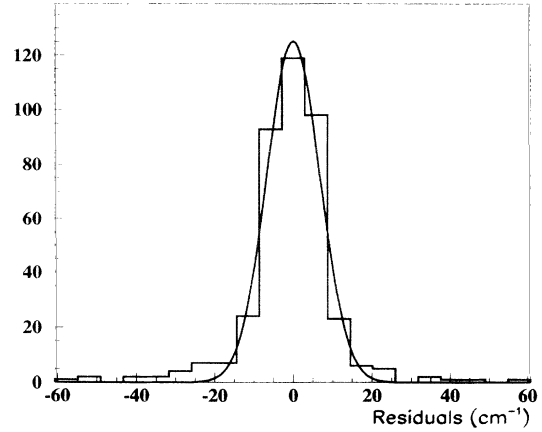

FIG. 4. Frequency distribution of residuals $(\alpha_{\mathrm{exp}} - \alpha_{\mathrm{fit}})$. The probability density of a Gaussian noise is indicated by the solid line.

deposited at 143 °C and 266 °C. Finally, the IR absorption spectrum of each sample was investigated separately by analyzing three vibration regions: the stretching region (1850 cm^{-1} $\leq \omega \leq$ 2250 cm^{-1}), the bending region (800 cm^{-1} $\leq \omega \leq$ 1000 cm^{-1}) and the wagging region (550 cm^{-1} $\leq \omega \leq$ 800 cm^{-1}) . The $\alpha(\omega)$ curve around each absorption region was fitted by minimizing the χ^2 function with respect to variations in the vector of the parameters a, that is

$$\chi^2 = \sum_{i=1}^{N}\left[\frac{\alpha(\omega_i) - f(\omega_i, a)}{\sigma_i}\right]^2, \qquad (2.3)$$

where σ_i is the estimated uncertainty of the absorption measurement corresponding to the wave number ω_i. The fitting function $f(\omega_i, a)$ is the superposition of two Gaussian functions having six free parameters, i.e., amplitudes, mean values and standard deviations, which are the components of the parameter vector a. The deconvolution procedure was carried out by application of the MINUIT program[13] which gives the estimates of both the numerical values of the parameters minimizing the χ^2 function and the relevant standard deviation; a typical deconvolution result is illustrated in Fig. 3 for the 2000–2100 cm^{-1} doublet, whereas the histogram in Fig. 4 shows the frequency distribution of the residuals and indicates that noise can be considered Gaussian.

Finally, the optical gaps were determined by means of Tauc's plots and the absorption coefficients in the low absorption region were measured by the photothermal deflection spectroscopy technique,[14] in order to obtain Urbach's energy and the gap DOS. Density was measured by floating the samples in tetrabromoethane, as described by Manfredotti *et al.*[3]

III. RESULTS AND DISCUSSION

The present section is organized in the following way. The first part describes the determination of the hydrogen content by an analysis of the wagging and stretching

IR modes. In the second part, the IR spectral analysis is extended to the bending region. The third section deals with the correlation of optical and structural properties with the deposition parameters, and focuses attention on the deposition temperature.

A. Hydrogen content and the wagging and stretching modes

The total hydrogen content (N_H) was determined from the IR stretching modes at 2000 cm^{-1} and at 2100 cm^{-1} through the following expression:[9]

$$N_H = A_{2000}I_{2000} + A_{2100}I_{2100}, \qquad (3.1)$$

where the integrals $I = \int [\alpha(\omega)/\omega]\, d\omega$ extend to the frequency range of the corresponding absorption mode.

The values of the two proportionality constants $[A_{2000} = (7.4 \pm 1.0) \times 10^{19}$ cm^{-2} and $A_{2100} = (2.1 \pm 0.2) \times 10^{20}$ $cm^{-2}]$ were previously obtained by our research group on low pressure CVD samples by correlating the IR data with the amount of hydrogen bound to Si, as determined by elastic-recoil-detection analysis (ERDA).[9]

Recently, Langford et al.[10] stated that the absorption strength of the stretching modes does not depend on the detail of sample preparation; they obtained consistent values of $A_{2000} = (9.0 \pm 1.0) \times 10^{19}$ cm^{-2} and $A_{2100} = (2.2 \pm 0.2) \times 10^{20}$ cm^{-2} by calibration of the IR integrated absorbances with the H content determined by means of nuclear reaction analysis (NRA) on plasma assisted CVD (PACVD) and reactive magnetron sputtered (RMS) samples.

The validity of our fitting procedure and of hydrogen content evaluation can be verified by examining Fig. 5 which shows the correlation between N_H [as calculated by Eq. (3.1)] and the integrated absorbance I_{640} of the
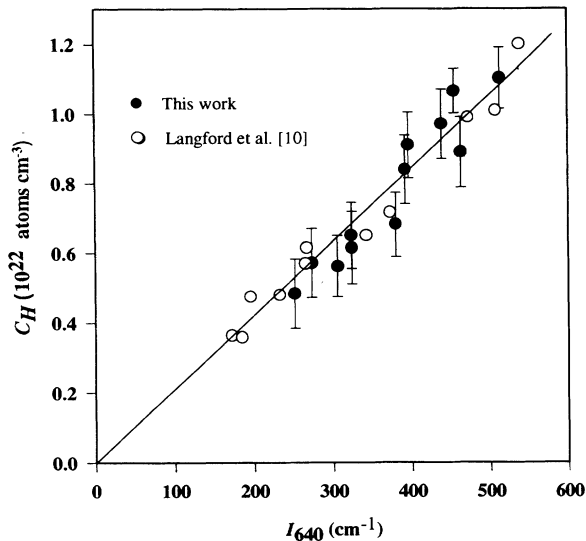

FIG. 5. Hydrogen content (N_H) vs the integrated absorbance I_{640} of the 640 cm^{-1} mode. Least-squares fit to data yields zero intercept and $A_{640} = (2.1 \pm 0.2) \times 10^{19}$ cm^{-2} slope.

wagging mode. Our data lie, within the estimated uncertainty, around the straight line obtained by Langford et al.[10] by calibrating the hydrogen content from NRA vs the integrated absorbance of the 640 cm^{-1} wagging mode for PACVD and RMS films. This fitting line has zero intercept and angular coefficient $A_{640} = (2.1 \pm 0.2) \times 10^{19}$ cm^{-2}.

According to the most common interpretation of the IR spectra,[6,10] absorption around 2000 cm^{-1} is attributed to the isolated and/or clustered SiH bonds and absorption around 2100 cm^{-1} is attributed to SiH_2 and/or to clustered SiH bonds. Since statistical fluctuation prevented us from having clear evidence of peaks centered around 2140 cm^{-1}, we have not considered the presence of SiH_3 bonds.

The peak due to SiH bond stretching occurs at 2003 $\pm$ 2 cm^{-1} and shifts by about 100 cm^{-1} with respect to the frequency shift of the isolated monohydride. This frequency shift value was obtained experimentally by Amato et al.[9] and by Langford et al.[10] and theoretically by Cardona,[6] who suggested that such frequency shift is due to the depolarizing field produced by a vibrating dipole in a cavity. The connection between frequency shift and depolarizing field is expressed by the following relation:

$$\Delta\omega = -\frac{1}{32\pi^3\epsilon_0 c^2\mu}\frac{e^{*2}}{R^3\omega_{2000}}\frac{\epsilon-1}{2\epsilon+1} \quad \text{[in SI units]}, \qquad (3.2)$$

where ϵ_0 and ϵ are the dielectric constants of the vacuum and of the a-Si matrix ($\epsilon = 12$), c is the velocity of light, and μ the reduced mass of the dipole. The radius, R, of the spherical cavity is assumed to be equal to the covalent radius of silicon[6] and the dynamical charge $e^* = 0.4e$ was calculated from the constant A_{2000} by the formula,

$$e^{*2} = \frac{4c^2\epsilon_0 n\mu\omega_{2000}}{A_{2000}} \quad \text{[in SI units]}, \qquad (3.3)$$

where n is the static refractive index of the material ($n = 3.42$). As regards the SiH_2 stretching band, the mean value saturates at $\omega_{2100} = 2080$ cm^{-1} which corresponds to a frequency shift $\Delta\omega = 48$ cm^{-1} with respect to the isolated di-hydride, which is in good agreement with the value ($\Delta\omega = 41$ cm^{-1}) calculated via the above mentioned model.[6,9]

B. Bond bending region

Figure 6 shows the close linear correlation between the 880 cm^{-1} and the 2100 cm^{-1} integrated absorbances. It is a direct verification of the commonly adopted interpretation[1,2] which attributes one of these two modes to the SiH_2 scissors bending and the other to the stretching mode. In addition, from the linear least-squares fit of data in Fig. 6, the proportionality constant between I_{2100} and I_{880} is 0.37±0.06. Such a value is in good agreement with the proportionality constant (0.38) evaluated by Shanks et al.[8] which refers to sputtering-prepared samples of a-Si:H.
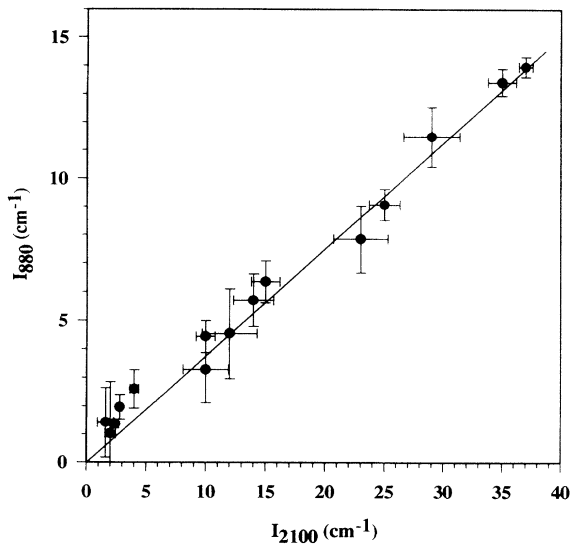
FIG. 6. Integrated absorbance I_{880} of the 880 cm^{-1} scissors-bending mode vs the integrated absorbance I_{2100} of the 2100 cm^{-1} SiH$_2$ stretching mode. Least-squares fit to our experimental data yields zero intercept and a slope of 0.37±0.07.

FIG. 8. Infrared absorption wave-number shift for peaks near 840 cm^{-1} (○) and 880 cm^{-1} (●).

The behavior of the integrated absorbance I_{840} of the 840 cm^{-1} mode vs I_{2100} is shown in Fig. 7. Its clearly nonlinear behavior can be interpreted through the model of Lucovsky and co-workers,[2,7] which assumes that the relatively strong absorption at almost 840 cm^{-1} is due only to near-neighboring pairs of SiH$_2$ groups or to longer chain segments (SiH$_2)_n$, whereas isolated SiH$_2$ groups are assumed to produce weak IR absorption at 840 cm^{-1} and strong absorption at 880 and 2100 cm^{-1}. The (SiH$_2)_n$ chain formation also provides an explanation for absorption-peak shifts for the peak near 880 cm^{-1}, as shown in Fig. 8. At low hydrogen concentrations (i.e., with low I_{2100} values) there is no evidence of absorption near 840 cm^{-1}, while an evident peak occurs at 875 cm^{-1}, which is generally assigned to the isolated SiH$_2$ scissors-
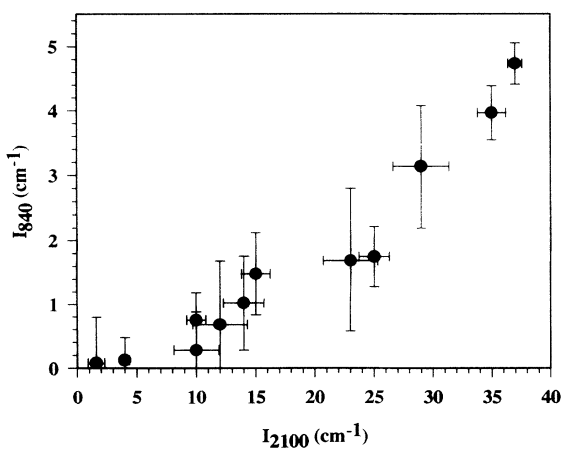
bending mode.[2] As the hydrogen content increases, two peaks appear, one at 842 cm^{-1} and the other at 885 cm^{-1} , which correspond to (SiH$_2)_n$ wagging and (SiH$_2)_n$ or SiH$_2$ scissors-bending modes, respectively.

C. Structural and optical properties

The above described IR spectral analysis, if related to deposition parameters and density measurements, can give some qualitative information on the microstructure of the material. The fractions of hydrogen bound as SiH and SiH$_2$ are given by the relationships $C_H(\text{SiH}) = A_{2000}I_{2000}/5 \times 10^{22}$ and $C_H(\text{SiH}_2) = A_{2100}I_{2100}/5 \times 10^{22}$, where the denominators represent the atomic density of

FIG. 7. Integrated absorbance I_{840} of the 840 cm^{-1} bending mode vs the integrated absorbance I_{2100} of the 2100 cm^{-1} SiH$_2$ stretching mode.
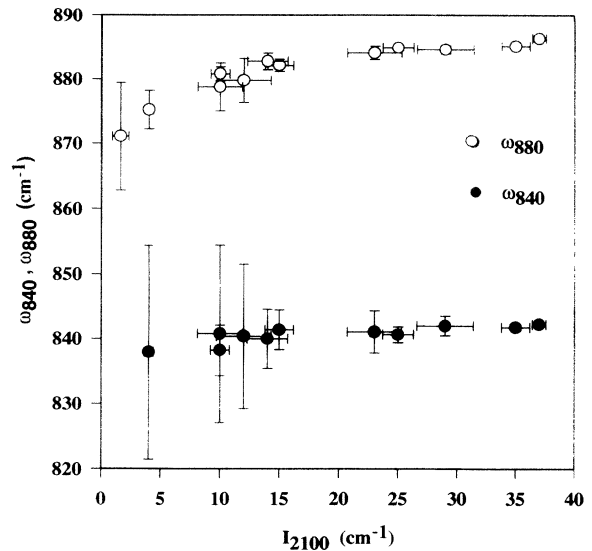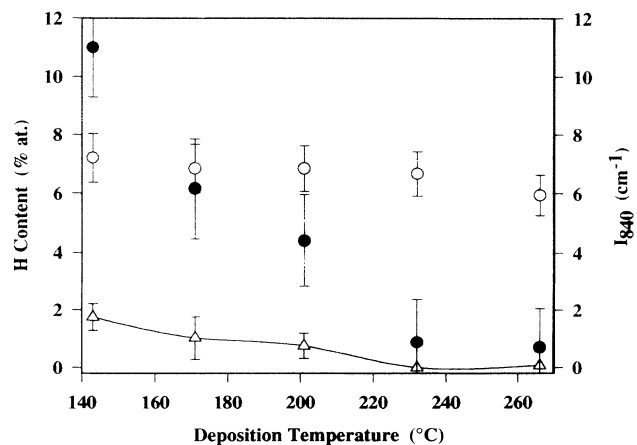

FIG. 9. Hydrogen concentration bound as SiH$_2$ (●) and SiH (○) as functions of the deposition temperature for a fixed deposition time (180 min). The symbols (△) refer to the values of I_{840}.
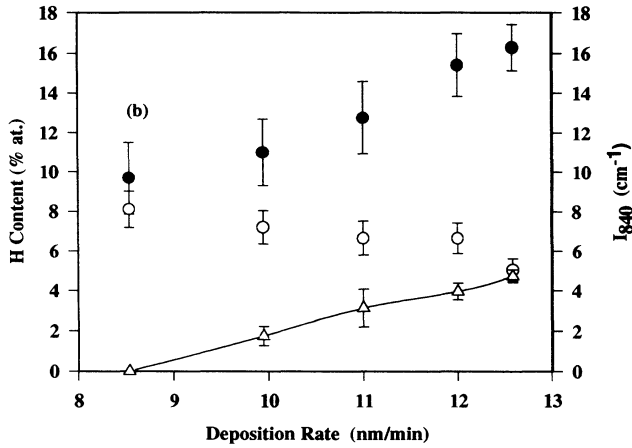
FIG. 10. Hydrogen concentration bound as SiH_2 (•) and SiH (o) as functions of deposition rate at a fixed deposition temperature (143 °C). The symbols (△) refer to the values of I_{840}.

crystalline silicon as reported in the literature.[10] Their values are shown in Figs. 9 and 10 as functions of the variable deposition parameters, i.e., deposition temperature and growth rate. It is worth noting that the H content in SiH groups ranges between 6 at.% and 8 at.%, whereas the hydrogen bound as SiH_2 covers a larger range of values from 1 at.% to 17 at.% so that we shall consider only SiH_2 as the independent variable of our analysis. Figures 9 and 10 show also the behavior of I_{840} as a function of deposition parameters; I_{840} will be considered, as already indicated, proportional to the number of $(SiH_2)_n$ chains. An increase in the deposition temperature or, similarly, a decrease in the deposition velocity, causes remarkable decrease of both SiH_2 and $(SiH_2)_n$ polymers, as already pointed out by Meiling et al.,[15] while the SiH content remains approximately constant.
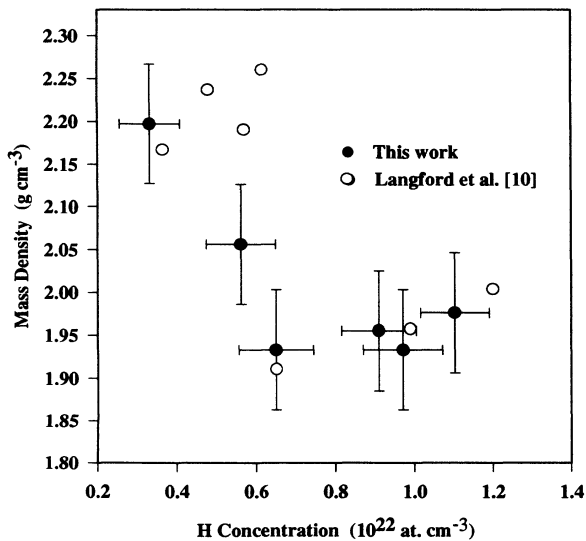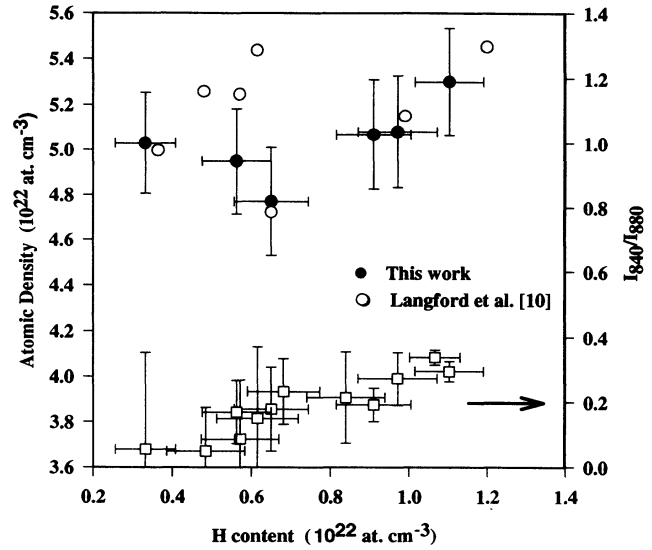

FIG. 12. Atomic densities (•) as functions of total hydrogen content. The open squares (□) indicate the I_{840}/I_{880} ratio.

Figures 11 and 12 show the mass density (ρ) and the atomic density of a-Si:H films as functions of the total hydrogen content; the trend of our experimental data is in agreement with the data reported by Langford et al.[10] We estimated the total atomic density N_{tot} from the measured mass density[3] and from the absolute atomic density of hydrogen [calculated from equation (3.1)] via the following expression:

$$N_{tot} = \rho \frac{N_A}{P_{Si}} + N_H \left(1 - \frac{P_H}{P_{Si}}\right) , \qquad (3.4)$$

where N_A is the Avogadro constant and P_H , P_{Si} are the molar mass of hydrogen and silicon, respectively.

FIG. 11. Mass densities (•) as function of total hydrogen content.

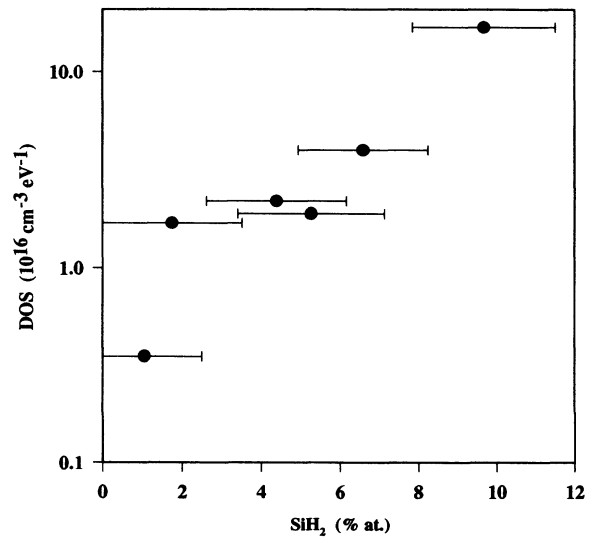FIG. 13. Gap density of states as a function of the SiH_2 content.

At a low hydrogen concentration, i.e., $N_H \leq 6-7 \times 10^{21}$ at. $\%/cm^3$, approximately corresponding to 5 at. % and 6 at. % hydrogen bound as SiH and SiH_2 respectively, the total atomic density slightly decreases and no $(SiH_2)_n$ chains, i.e., no absorption peaks near 840 cm^{-1} form. This means that only isolated SiH and SiH_2 bonds are present and that the average intersilicon distance increases.[15]

As soon as the I_{840}/I_{880} ratio, indicated by open squares ($\square$) in Fig. 12, is no longer negligible, i.e., when $(SiH_2)_n$ chains begin forming, the atomic density considerably increases; this phenomenon may be due to the formation of microcavities. With cavity increase, hydrogen atoms are no longer incorporated as isolated SiH or SiH_2 bonds but they presumably "decorate" the surfaces of the microcavities[15,16] and/or increase the length of the $(SiH_2)_n$ chains, as suggested by the slightly higher I_{840}/I_{880} ratio.[4] In addition, the constant mass density indicates that the intersilicon distance remains constant because the hydrogen in excess is incorporated in the microcavities.

It must be noted that the lowest atomic density occurs at a deposition temperature of $\sim 170\,^\circ C$, which is a threshold temperature below which hydrogen is incorporated as SiH and/or SiH_2 bonds and above which hydrogen is incorporated in microcavities or in $(SiH_2)_n$ chains. However, the value of this threshold temperature is not to be considered absolute since hydrogen incorporation depends also on deposition rate as shown in Fig. 10.

Such an interpretation of the behavior of density as a function of the hydrogen content is corroborated by the model described by Street[17] which ascribes SiH_2 group formation to surface reaction kinetics, where two radicals SiH_3 bind to the network close to each other, so that one H atom in each group may be released to form H_2 molecules and the two resulting dangling bonds may rearrange themselves and restore the coordination of silicon atoms. The relatively small density at high SiH_2 content may be explained by the fact that our samples were obtained at low temperatures ($\leq 170\,^\circ C$) or at high deposition rates, that is when no structural balancing occurs[17] and the formation of a cavity around the SiH_2 bonds or $(SiH_2)_n$ chains results in the only possible topological configuration.[16] As the SiH_2 content decreases, at deposition temperatures below $170\,^\circ C$, hydrogen diffusion favors a network rearrangement and a resulting reduction of microcavities in the material. We point out that our thermovolumetric and thermogravimetric measurements have given some evidence of hydrogen effusion at $170\,^\circ C$, probably due to the breaking of the SiH_2 bonds. Another indirect evidence of the strict correlation between the SiH_2 or $(SiH_2)_n$ content and the structural disorder of the material is shown in Figs. 13 and 14, in which the density of states and Urbach's slope, E_0, are plotted vs the SiH_2 content. Hydrogen bound as SiH_2 tends to increase the structural disorder in terms of bond-angle distribution and consequently to increase both Urbach's energy and the density of states in the gap. The behavior of the optical band gap E_G is shown as a function of the hydrogen bound as SiH_2 content in Fig. 15, which displays a noticeable enlargement of the optical gap as
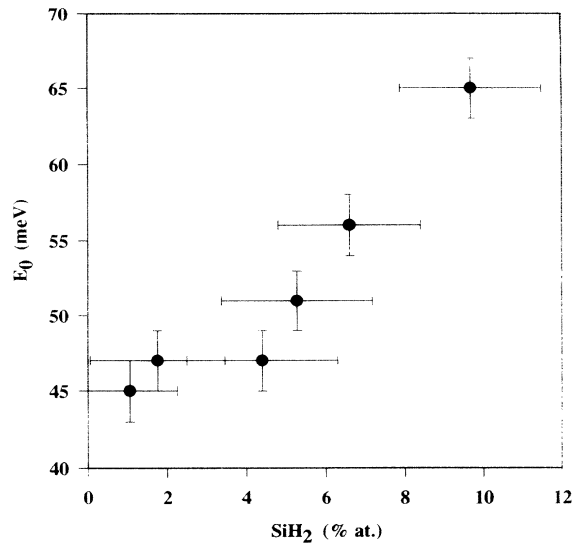

FIG. 14. Urbach's energy E_0 as a function of the SiH_2 content.

a function of SiH_2 as is qualitatively shown by Maessen et al.[18]

The fact that E_G, gap DOS and E_0 increase monotonically as functions of the SiH_2 content allows us to conclude that the increase of the pseudogap is not caused by progressive removal of defect states in the gap or by disorder, but by the increasing influence of hydrogen bonds on the a-Si:H structure. Since at high hydrogen concentration SiH units are progressively replaced by SiH_2 and $(SiH_2)_n$ polysilane chains showing effective gaps[5] of 4–6.5 eV, the mentioned optical measurement values can be explained if a-Si:H films are considered a mixture of two binary Si:H alloys: one has a constant SiH bonds concentration and small energy gaps; the other has wide gap polysilane chains whose growing number or length
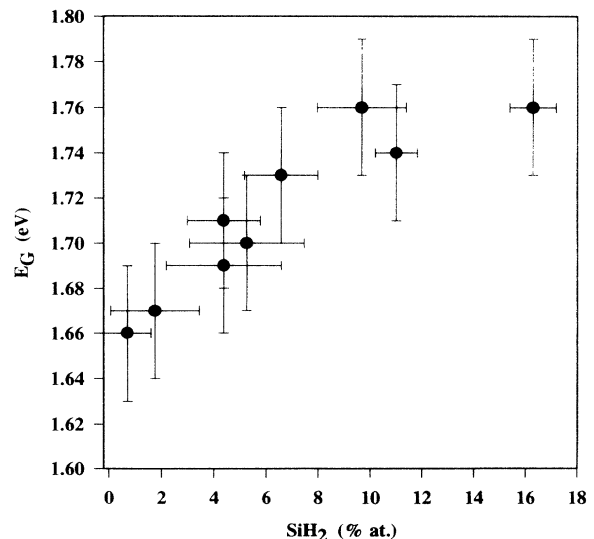

FIG. 15. Optical energy gap E_G as a function of the SiH_2 content.

enlarges the average gap and, at the same time, increases structural disorder.

IV. CONCLUSIONS

We have investigated the effect of hydrogen incorporation as SiH, SiH_2, $(SiH_2)_n$ on the optical and structural properties of a-Si:H samples deposited by PECVD. The total hydrogen content was obtained through the determination of the absorption strength of 2000–2100 cm^{-1} stretching modes. The good agreement of our data with the calibration line obtained by NRA and ERD measurements corroborates our results.

The absorption strength of the peaks at 880 cm^{-1} shows a linear correlation with the absorption strength at 2100 cm^{-1} and indicates that the 880 cm^{-1} absorption peak related to the scissors-bending mode of the SiH_2 group is in agreement with previously assigned values. The I_{880}/I_{2100} ratio obtained from a least-squares linear fit is 0.37 ± 0.06.

The nonconstancy of the value of the peak frequency of the scissors mode and the nonlinear behavior of I_{840} as a function of I_{2100} have been attributed to the formation of $(SiH_2)_n$ groups. Such polysilane chains are responsible for the formation of microcavities, as results from an analysis of the atomic and mass-density curves as functions of the incorporated-hydrogen concentration. These results led us to identify two different processes of hydrogen incorporation. Isolated SiH and SiH_2 bonds occur when the hydrogen content is below 10 at. %, whereas with higher hydrogen concentrations the formation of $(SiH_2)_n$ chains cause the formation of empty cavities where hydrogen is preferentially incorporated. In our samples these two processes developed at deposition temperatures above and below a threshold value of 170 °C, which should not be believed unique under any deposition condition, since hydrogen incorporation depends to a great extent on the deposition rate.

Finally, we observed a monotonic increase in the gap density of states, in Urbach's energy and in the optical band gap vs the SiH_2 bond concentrations, such increase suggesting that high hydrogen concentrations give rise to defects and disorder in the material. The material is then to be considered a mixture of ordinary small band gap a-Si:H having a constant amount of SiH bonds (4–7 at. %) and wide band gap polysilane chains, whose net effect results in a "positive" enlargement of the average band gap.

[1] M. H. Brodsky, M. Cardona, and J. J. Cuomo, Phys. Rev. B **16**, 3556 (1977).

[2] G. Lucovsky, R. J. Nemanich, and J. C. Knights, Phys. Rev. B **19** , 43 (1980), **19**, 2064 (1980).

[3] C. Manfredotti, F. Fizzotti, M. Boero, P. Pastorino, E. Vittone, and V. Rigato, in *Amorphous Silicon Technology*, edited by E. A. Schiff, M. J. Thompson, A. Madan, K. Tanaka, P. G. LeComber, MRS Symposia Proceeding No. 297 (Materials Research Society, Pittsburgh, 1993), p. 231.

[4] S. Furukawa and N. Matsumoto, Phys. Rev. B **31**, 2114 (1985).

[5] D. J. Wolford, B. A. Scott, J. A. Reimer, and J. A. Bradley, Physica **117B-118B**, 920 (1983).

[6] M. Cardona, Phys. Status Solidi B **118**, 463 (1983).

[7] W. B. Pollard and G. Lucovsky, Phys. Rev. Lett. **26**, 3172 (1982).

[8] H. Shanks, C. J. Fang, L. Ley, M. Cardona, F. J. Demond, and S. Kalbitzer, Phys. Status Solidi B **100**, 43 (1980).

[9] G. Amato, G. Della Mea, F. Fizzotti, C. Manfredotti, R. Marchisio, and A. Paccagnella, Phys. Rev. B **43**, 6627 (1991).

[10] A. A. Langford, M. L. Fleet, B. P. Nelson, W. A. Lanford, and N. Maley, Phys. Rev. B **45**, 13 367 (1992).

[11] A. Madan, P. Rava, R. E. I. Schropp, and B. von Roedern, Appl. Surf. Sci. **70/71**, 716 (1993).

[12] N. Maley, Phys. Rev. B **46**, 2078 (1992).

[13] F. James and M. Roos, CERN D506 MINUIT Manual, Release 89.12J (1989).

[14] W. B. Jackson and N. M. Amer, *Optical Properties of Defect States in a-Si:H in Semiconductors and Semimetals*, Part B (Academic Press, New York, 1984), Vol. 21.

[15] H. Meiling, M. J. Van Den Boogard, R. E. I. Schropp, J. Bezemer, and W. F. Van Der Wef, in *Amorphous Silicon Technology*, edited by P. C. Taylor, M. J. Thompson, P. G. LeComber, Y. Hamakawa, and A. Madan, MRS Symposia, Proceedings No. 192 (Materials Research Society, Pittsburgh, 1990), pp. 645–650.

[16] W. Y. Ching, D. J. Lam, and C. C. Lin, Phys. Rev. B **21**, 2378 (1980).

[17] R. A. Street, *Hydrogented Amorphous Silicon* (Cambridge University Press, Cambridge, 1991).

[18] K. M. H. Maessen, M. J. H. Pruppers, J. Bezemer, F. H. P. H. Habraken, and W. F. van der Weg, in *Amorphous Semiconductors Pure and Hydrogenated*, edited by A. Madan, M. Thompson, D. Adler, and Y. Hamakawa, MRS Symposia Proceedings No. 95 (Materials Research Society, Pittsburgh, 1989), p. 201.